Effective Image and Spectral Data Acquisition Method Used in Scanning Near-field Optical Microscopy by Bimorph-based Shear Force Sensor

Wei Cai, Mu Yang, Yingjie Wang, and Guangyi Shang*
Department of Applied Physics
Beihang University, BUAA
Beijing, China
*e-mail: gyshang@buaa.edu.cn

Abstract—**We have introduced a home-made scanning near-field optical microscope (SNOM) with bimorph-based shear force sensor. The instrumentation of the imaging system and the key techniques such as the bimorph-based non-optical shear force sensor design and the fabrication of optical fiber probes used in this SNOM are described in details. Then the good performance of the system is demonstrated by various experiments such as shear force imaging, near-field optical imaging, surface plasmon resonance detection, and near-field spectroscopy. The imaging and spectroscopic experimental results suggest that this home-made SNOM and bimorph-based shear force detection method would be promising techniques to be used in a variety of nanomaterials research and their optical applications.**

Keywords—scanning near-field optical microscopy; shear force microscopy; bimorph shear force sensor; near-field spectroscopy

I. INTRODUCTION

Scanning near-field optical microscope (SNOM) has proven to be one of the most powerful image systems and techniques to explore the optical field in nanoscale [1, 2]. It can be used to observe the surface topographic and optical properties of the material with the resolution breaking the classical optical diffraction limit. The working principle of SNOM is utilizing a sharp tip to detect the light in the near-field of the test sample point by point. Thus, the resolution of SNOM is only restricted by the tip aperture size (tip curvature for apertureless SNOM) and the tip-sample separation. Nowadays SNOM has been widely used in nanooptics, nanophotonics, and plasmonics research. From the aspect of instruments, the breadth of SNOM applications depends mainly on the imaging technical progress. One of the critical techniques in SNOM is to control the tip position to be several nanometers closer to a sample surface. Various feedback mechanisms of tip-sample distance control have been employed, including electron tunneling current [3], atomic force [4], and non-optical shear force detection [5].

At present non-optical shear force detection has been the most popular tip-sample distance regulation method in SNOM experiments. In this method, the small amplitude of a dithered tip damps rapidly when the tip approaches the sample surface due to the shear force interaction. So by monitoring the tip vibration, the tip-sample distance can be controlled precisely.

Typical non-optical shear force detection is realized by using a commercially available quartz tuning fork, operated at the resonance frequency of the tip-fork assembly [6]. Compared with optical scheme, the measurement of the amplitude of tip oscillation is very simple by using tuning fork. The induced electrical signal by the piezoelectric effect is proportional to the fork deformation [7]. However, sticking the fiber to the fork is a difficult task because the resonance frequency of the tuning fork is very sensitive to the glue [8]. In addition, the quality factor of the tuning forks is high, resulting in slow scan rates of imaging. To overcome those problems, our group presents a piezoelectric bimorph shear force sensor and it is successfully used for SNOM system [9, 10].

In this article, we firstly describe the instrumentation of the imaging system and the key techniques in our home-made bimorph-based SNOM. This versatile instrument has different operation modes for near-field optical imaging. For example, working in the reflection-collection mode or tip-illumination mode can be easily achieved. By adding some specially designed accessories such as semi-cylinder prism sample stage and light path couplers, detecting the surface plasmon resonance (SPR) and capturing spectra in near-field can also be realized. Then the good performance of the system is demonstrated by various applications such as shear force imaging, near-field optical imaging, SPR detection, and near-field spectroscopy.

II. INSTRUMENTATION

A. Shear force sensor design

The shear force sensor used in our experiment mainly consists of a piezoelectric bimorph cantilever, which has two piezoelectric layers and one conductive middle shim layer [9-11]. A picture of commercially available piezoelectric bimorph is showed in Fig. 1(a). The model of the shear force sensor can be simply described by the theory on cantilever elastic deformation [12]. In all our experiments, this model is adopted. The measured parameters of the force sensor coincide well with the calculated values. Two important design formulas are given as below. The static spring constant k_0 of the sensor can be estimated by

$$k_0 = Ewt^3 / 4l^3 \qquad (1)$$

where E is the Young's modulus, l the length, w the width, and t the thickness respectively. The fundamental resonance f_0 of the sensor is described by

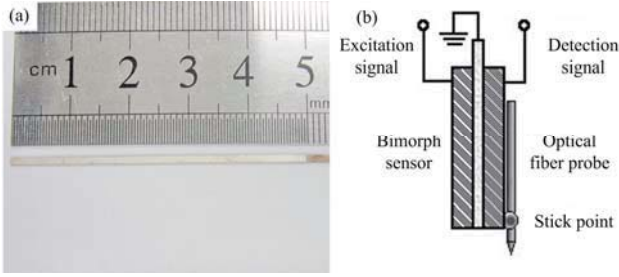$$f_0 = (\eta_0^2 / 2\pi)(t / l^2)(E / 12\rho)^{1/2} \qquad (2)$$

Fig. 1. (a) A picture of commercially available piezoelectric bimorph. (b) Schematic of bimorph-based shear force sensor.

where $\eta_0 = 1.875$ and ρ is the mass density. Typical parameters of bimorph used in experiments are $l = 6$ mm, width $w = 1$ mm, thickness $t = 0.6$ mm, Young's modulus $E = 5.2 \times 10^{10}$ N/m^2, density $\rho = 6500$ kg/m^3. The spring constant k_0 and the resonance frequency f_0 can be calculated theoretically by using above formulas.

The connections of the sensor are shown in Fig. 1(b). The middle brass electrode layer is ground. The left side piezo layer is used as a dither piezo and electrically connected to an excitation signal. A constant-frequency sine wave is applied to it to drive the bimorph to vibrate parallel to the sample surface. Meanwhile the right side piezo layer will generate an induced piezo voltage when driving at its resonance frequency. The induced voltage is enhanced by using a preamplifier and then demodulated by the lock-in amplifier. When the tip goes down and approaches the sample surface, the oscillation of the bimorph is damped due to the tip-sample shear force interaction, resulting in a decrease in the output signal of the lock-in amplifier. The amplitude of the decreased signal is compared with a set-point of the feedback circuit and used to control the tip-sample distance during scanning.

The force F detected by the shear force sensor can be estimated by $F = (1 - V/V_0)k_0x_0 / \sqrt{3}Q$, where x_0 is the vibration amplitude far away from a sample, Q is quality factor defined as f_0/f, f is the full width at half maximum, V is the amplitude of the detection piezo voltage, and V_0 is maximum value [5]. This formula suggests that the force detected by the sensor or the sensitivity of the shear force sensor can be further optimized by increasing the Q factor [13] or minimizing the spring constant k_0, which will be discussed in details in another paper.

B. Optical fiber probe

Single mode optical fibers with outer diameter of 125 μm have been used to prepare optical fiber tips. The tips are fabricated by the chemical etching device developed in our laboratory based on Turner method [14]. In this method, fibers without cladding are dipped vertically into the etching solutions which consist of 40% hydrofluoric (HF) acid solutions covered by organic solvent as a protecting layer. The role of the protecting layer is to prevent evaporation of toxic HF and protect the taper from further etching after the tip formation. The reason for tip formation is that a meniscus of the HF solution is formed due to the surface tension difference between the HF solution and the solvent cover [15]. The angle of the tip strongly depends on the solvent cover. By changing the type of the solvent, the tip angle varies from 8° to 41° [16].
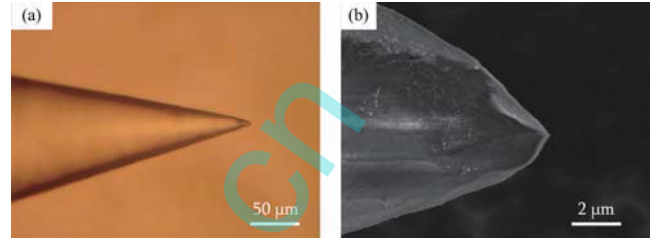

Fig. 2. (a) An optical image and (b) a typical scanning electron microscope (SEM) image of a fiber tip.

By carefully selecting the organic solvent used as the cover layer (e.g., cyclohexane), the fiber tips can be fabricated with reproducible shapes and sizes. The processes of the chemical reaction are carried out in a plastic petri dish. The etching time is ~120 min at room temperature. The tips are then washed with deionized water. Fig. 2 shows an optical image and a typical scanning electron microscope (SEM) image of a fiber tip. The taper angle is about 40°, ensuring high mechanical stiffness and optical signal efficiency. The fiber tip is then carefully attached to the free end of the bimorph along its longitudinal axis with a drop of superglue, forming a shear force sensor.
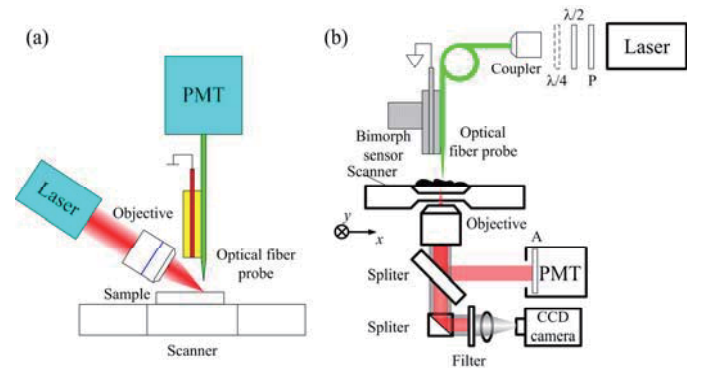
C. Configuration of the set-up

Fig. 3. Schematics of the system configurations: (a) reflection mode and (b) transmission mode. The light source and the detector can be exchanged with each other by adding some accessories.

Our home-made SNOM system operating in reflection and transmission mode has been built based on the bimorph shear

force sensor. The schematics are shown in Fig. 3. The sample can be mounted on a home-made flat scanner (The scan range is ~30 μm×30 μm×15 μm) [17] or a 3D nano positioning stage (P517.3CL, Physik Instrumente, Germany, the scan range is 110 μm×110 μm×20 μm). The laser with 632 nm wavelength and 3 mW power passes through the objective lens (SLMPlan 50x/N.A.= 0.45, Olympus, Japan) and focuses on the sample surface. In section III D, the source can also be changed to xenon arc lamp for spectroscopic research. The near-field optical signal is collected by the fiber tip and detected by the photomultiplier tube (PMT, CR131, Hamamatsu, Japan). A commercially available SPM controller (CSPM5000, BenYuan Nano-Instruments Ltd., China) is used, which has the abilities of reference signal generation, lock-in measurement, feedback control, x-y scan signal, and data acquisition. A low-noise current preamplifier (SR570, Stanford Research Systems, USA) is employed to detect the photocurrent from the PMT. It is also possible to accomplish a tip-illumination measurement mode by exchanging the positions of the laser and the PMT detector with each other and adding some accessories.

III. APPLICATIONS

A. Shear force imaging

The performance of the system is firstly characterized by shear force imaging. The test sample is prepared in the following steps. Firstly, latex spheres are dispersed on a clean glass substrate. Then Cd film is produced on glass by evaporation. Finally holes are formed by removing latex spheres with the method of calcination. Fig. 4(a) shows a typical shear force image of the test sample with the scan range of 2.2 μm×2.2 μm, obtained at the set-point ~0.95 of the maximum vibration amplitude and the line scan rate of 0.5 Hz. In the image, a number of individual holes of about 220 nm in diameter can be seen clearly. The imaging resolution is ~30 nm which can be estimated by the cross-section line showed in Fig. 4(b). These results show excellent performance both in sensitivity and in stability.
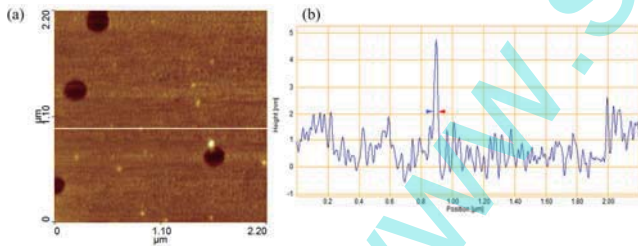

Fig. 4. (a) Test sample is Cd film deposited on glass substrate, a number of individual holes and particles distribute evenly on the film. (b) The cross-section line in (a).

B. Near-field optical imaging

The stable shear force imaging is the basis of optical imaging. Then we give two examples to demonstrate the ability of optical image acquisition. The first example (Fig. 5) shows the topographic and optical images of a CD-R surface obtained simultaneously at the same pre-set parameters in reflection mode. The scan area is 20 μm×20 μm. This result suggests the

system also has the ability to obtain optical images. After carefully comparing the two images, we find out that the contrasts of the two images are reverse. One possible explanation is that the reflectivities of the groove tops and bottoms are different. From the optical image, the groove bottoms have better reflectivity.
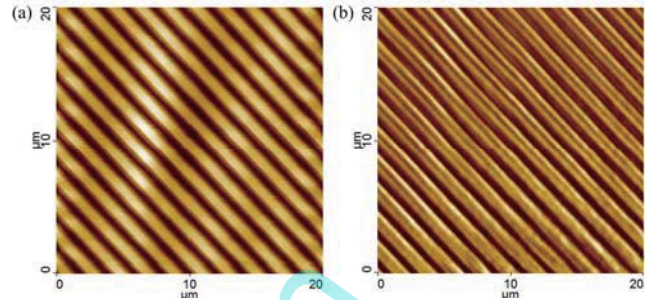

Fig. 5. (a) Shear force topographic image and (b) near-field optical image of a CD-R sample obtained simutainously in reflection mode.

The second example (Fig. 6) gives the topographic and optical images of a test grating (SNG01, NT-MDT, Russia) obtained simultaneously in transmission mode. This sample has a regular structure of vanadium film (10 nm thick) deposited on a quartz (SiO_2) substrate. In the experiment, the set-point is ~0.95 of the maximum vibration amplitude and the line scan rate is 0.5 Hz. The scan area is 25 μm×25 μm. In the topographic image, the rhomb shaped metal films and some small particles are clearly presented. In the corresponding optical image, the rhomb area is darker which illustrates that the metal films have higher optical absorptivity than surrounding areas.
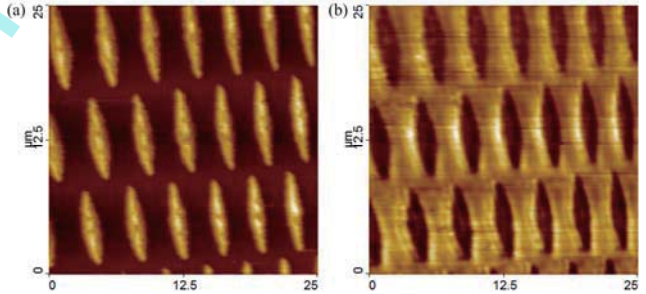

Fig. 6. (a) Shear force topographic image and (b) near-field optical image of a SNOM test grating obtained simutainously in transmission mode.

C. Surface plasmon resonance detection

Since the bimorph-based shear force sensor is compact and reliable, our system can perform various experiments such as detecting the SPR in near-field besides imaging. Surface plasmon is a surface electromagnetic field confined to the near vicinity of the dielectric-metal interface [18]. In recent years, it has been extensively researched because of its potential applications in integration circuits, bio-sensors, and photovoltaic devices [19]. Conventional detecting method is to use the Kretschmann configuration to monitor the totally reflected light in far field. When SPR is excited, most energy of the incident light is coupled into the noble metal film due to the resonance energy transfer, which causes the reflected light

signal to reduce to the minimum [20]. Correspondingly, the near-field intensity would reach the maximum.

In order to implement SPR detection in near-field on our home-made system, a specially designed sample stage has been used which consists of a semi-cylinder prism and two mirrors. The light path has been modified to be very similar to commonly used Kretschmann configuration [21, 22]. While the incident angle continuously changes, the evanescent optical signal is collected by the fiber probe and detected by the photomultiplier tube.

Fig. 7(a) shows the typical results of a coverslip as a test sample. No matter what polarization state of the incident light is, no obvious resonance phenomenon arises. But we can still find that in this configuration the angle of total reflection is ~41.3°. The optical signals in the left part of the curves are higher. One possible explanation is that part of the refracted light enters into the taper side of the tip, which might cause the background level to increase. After the incident angle passes through the angle of total reflection, the intensity of the optical signal drops to almost zero drastically.

Then we use index matching oil to couple a gold-coating coverslip with the upper surface of the prism. The gold film is prepared by using a sputter-coater (KYKY SBC-12, Beijing, China). The thickness of the film is ~50 nm which is estimated by the coating current and the deposited time. Fig. 7(b) shows obviously that under the condition of the p-polarized incident light, the resonance phenomenon exists at ~43.5°. Accordingly, under the condition of s-polarized incident light, this phenomenon disappears. The above results are also consistent with the theory that the SPR resonance angle can be calculated analytically. In order to remove the background signal before reaching the SPR resonance angle, we use the s-polarized curve as the background and subtract it in p-polarized curve through interpolation algorithm before the resonance angle. The result showed in Fig. 5 (c) is more in agreement with the analytical or numerical simulation results.
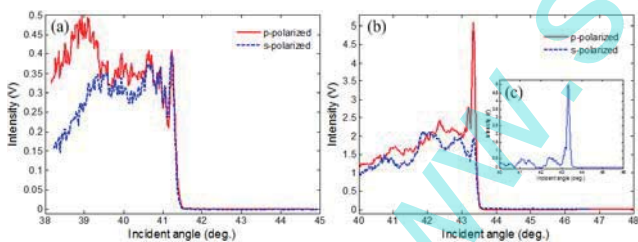

Fig. 7. Intensity curves detected in the near-field at different angle of incident light. (a) The test sample is a coverslip. (b) The test sample is a coverslip with gold coating. (c) The resonance curve is processed by subtracting the s-polarized curve (dash line) as background from the p-polarized curve (solid line) with interpolation algorithm.

D. Near-field spectroscopy with broadband excitation

SNOM can not only be used for optical imaging with nanometer resolution but also can be combined with the conventional optical spectroscope. As we know, optical spectroscopy plays an important role in researching the structure of matter. However, like optical imaging, its spatial resolution is also restricted by the diffraction limit. In SNOM, the spot size under the tip aperture is smaller than the wavelength. So the spatial resolution of optical spectroscopy can be extended into nanometers. With a series of techniques such as tip enhanced method, spectroscope can capture the Raman spectrum from a single dye molecule [23].

For researching surface plasmon polariton phenomenon in spectroscopic way, the light source in the system needs to be changed from a single wavelength source to a broadband excitation source [24, 25]. The selection of the broadband source's wavelength range is depended on the studied material's properties. For example, wavelength at the visible range is suitable for researching silver nanoparticles, and wavelength in the near-infrared region is appropriate for researching gold nanowires. Some groups use femtosecond laser pulses through a photonic crystal fiber to generate a supercontinuum source to meet the requirement of the spectroscopic measurements [26]. However, the femtosecond laser is rather costly. According to relevant literature, we find that xenon arc lamp (Xe lamp) is more commonly used and cheaper. Also Xe lamp has some advantages over supercontinuum source in power stability and spectral flatness [27].

In experiments, a 500 W Xe lamp system (CHF-XM500, Beijing Changtuo Co., China) is used as a broadband light source which is coupled into an inverted microscope with optical cable and home-made couplers. The optical signal focused on the sample surface with the objective is collected by the fiber probe and then sent to the grating spectroscope (Omni-λ500, Zolix Inc, China). Finally the spectrum is captured by the CCD detector (EMCCD, Newton DU970UVB, Andor).
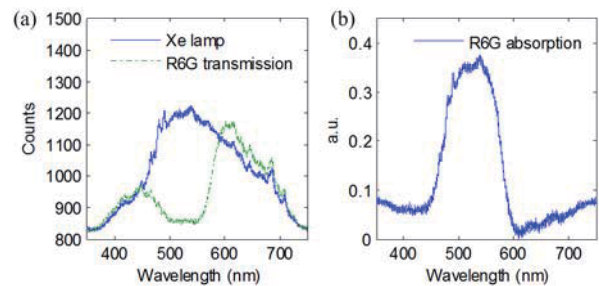

Fig. 8. (a) Near-field transmission spectrum of xenon lamp (solid line) and R6G test sample (dash line). The test sample is prepared with a coverslip substrate covered with a drop of R6G solution. (b) Absorption spectrum of R6G test sample.

In order to test our near-field spectroscopic system, we measure the absorption spectrum of Rhodamine 6G (R6G) sample. The sample is prepared by putting a drop of diluted R6G solution on a coverslip and then drying it in air. On current system, we need to measure two spectra to obtain absorption spectrum. Firstly, the near-field transmission spectrum of xenon lamp is measured and a clean coverslip is used as the sample. Secondly, the coverslip is replaced by R6G sample which is prepared with a coverslip substrate covered with R6G solution. Two spectra are showed in Fig. 8(a). Then, absorption spectrum of R6G is obtained by subtracting the

transmission spectrum from the source spectrum after normalization. The result is presented in Fig. 8(b) which is in accordance with Ref. [25]. This result demonstrates that our system has potential application prospect in measurement of the spectral properties such as scattering or absorption of noble metal nanoparticles in near-field.

IV. CONCLUSIONS

In conclusion, we have demonstrated a home-made SNOM system by using the bimorph based shear force sensor for tip-sample regulation. The good performance of the system is demonstrated by various applications such as shear force imaging, near-field optical imaging, SPR detection, and near-field spectroscopy. Consequently, our versatile near-field imaging system is expected to be effectively used in various fields.

REFERENCE

[1] B. Hecht, B. Sick, U. P. Wild, V. Deckert, R. Zenobi, O. J. F. Martin, and D. W. Pohl, "Scanning near-field optical microscopy with aperture probes: Fundamentals and applications," *The Journal of Chemical Physics,* vol. 112, pp. 7761-7774, 2000.

[2] J. Kim and K. Song, "Recent progress of nano-technology with NSOM," *Micron,* vol. 38, pp. 409-426, 2007.

[3] D. W. Pohl, W. Denk, and M. Lanz, "Optical stethoscopy: Image recording with resolution λ/20," *Applied Physics Letters,* vol. 44, p. 651, 1984.

[4] D. P. Tsai and W. K. Li, "Optical fiber structures studied by a tapping-mode scanning near-field optical microscope," *Journal of Vacuum Science & Technology A: Vacuum, Surfaces, and Films,* vol. 15, pp. 1427-1431, 1997.

[5] K. Karrai and R. D. Grober, "Piezoelectric tip‐sample distance control for near field optical microscopes," *Applied Physics Letters,* vol. 66, pp. 1842-1844, 1995.

[6] J. Rychen, T. Ihn, P. Studerus, A. Herrmann, K. Ensslin, H. Hug, P. van Schendel, and H. Guntherodt, "Operation characteristics of piezoelectric quartz tuning forks in high magnetic fields at liquid helium temperatures," *Review of Scientific Instruments,* vol. 71, pp. 1695-1697, 2000.

[7] Y. Qin and R. Reifenberger, "Calibrating a tuning fork for use as a scanning probe microscope force sensor," *Review of Scientific Instruments,* vol. 78, pp. 063704-7, 2007.

[8] P. Muhlschlegel, J. Toquant, D. W. Pohl, and B. Hecht, "Glue-free tuning fork shear-force microscope," *Review of Scientific Instruments,* vol. 77, pp. 016105-3, 2006.

[9] G. Y. Shang, C. Wang, J. Wu, C. L. Bai, and F. H. Lei, "Shear force scanning near-field optical microscope based on a piezoelectric bimorph cantilever," *Review of Scientific Instruments,* vol. 72, pp. 2344-2349, 2001.

[10] F. H. Lei, G. Y. Shang, M. Troyon, M. Spajer, H. Morjani, J. F. Angiboust, and M. Manfait, "Nanospectrofluorometry inside single living cell by scanning near-field optical microscopy," *Applied Physics Letters,* vol. 79, pp. 2489-2491, 2001.

[11] F. H. Lei, L. Huang, O. Piot, A. Trussardi, M. Manfait, G. Shang, and M. Troyon, "Active bimorph-based tapping-mode distance control for scanning near-field optical microscopy of biological samples in liquid," *Journal of Applied Physics,* vol. 100, p. 084317, 2006.

[12] D. Sarid, *Scanning force microscopy*: Oxford University Press, 1991.

[13] F. Lei and M. Manfait, "Non-optical bimorph-based force sensor for scanning near-field optical microscopy of biological materials: characteristics, design and applications," *Surface and Interface Analysis,* vol. 39, pp. 674-683, 2007.

[14] D. R. Turner, "Etch procedure for optical fibers," US Patent 4469554, 1984.

[15] A. Lazarev, N. Fang, Q. Luo, and X. Zhang, "Formation of fine near-field scanning optical microscopy tips. Part I. By static and dynamic chemical etching," *Review of Scientific Instruments,* vol. 74, pp. 3679-3683, 2003.

[16] P. Hoffmann, B. Dutoit, and R.-P. Salathé, "Comparison of mechanically drawn and protection layer chemically etched optical fiber tips," *Ultramicroscopy,* vol. 61, pp. 165-170, 1995.

[17] W. Cai, G. Shang, Y. Zhou, P. Xu, and J. Yao, "An alternative flat scanner and micropositioning method for scanning probe microscope," *Review of Scientific Instruments,* vol. 81, p. 123701, 2010.

[18] S. A. Maier, *Plasmonics: Fundamentals and Applications*. New York: Springer US, 2007.

[19] H. A. Atwater and A. Polman, "Plasmonics for improved photovoltaic devices," *Nature materials,* vol. 9, pp. 205-213, 2010.

[20] J. Homola, S. S. Yee, and G. Gauglitz, "Surface plasmon resonance sensors: review," *Sensors and Actuators B: Chemical,* vol. 54, pp. 3-15, 1999.

[21] O. Marti, H. Bielefeldt, B. Hecht, S. Herminghaus, P. Leiderer, and J. Mlynek, "Near-field optical measurement of the surface plasmon field," *Optics communications,* vol. 96, pp. 225-228, 1993.

[22] P. Dawson, B. Puygranier, and J. Goudonnet, "Surface plasmon polariton propagation length: A direct comparison using photon scanning tunneling microscopy and attenuated total reflection," *Physical Review B,* vol. 63, p. 205410, 2001.

[23] J. Steidtner and B. Pettinger, "Tip-Enhanced Raman Spectroscopy and Microscopy on Single Dye Molecules with 15 nm Resolution," *Physical Review Letters,* vol. 100, p. 236101, 2008.

[24] J. Seidel, S. Grafstrom, C. Loppacher, S. Trogisch, F. Schlaphof, and L. Eng, "Near-field spectroscopy with white-light illumination," *Applied Physics Letters,* vol. 79, pp. 2291-2293, 2001.

[25] N. Park, K.-D. Park, Y. Chung, and M. S. Jeong, "Scanning absorption nanoscopy with supercontinuum light sources based on photonic crystal fiber," *Review of Scientific Instruments,* vol. 82, pp. 123102-4, 2011.

[26] J. Bouillard, S. Vilain, W. Dickson, and A. Zayats, "Hyperspectral imaging with scanning near-field optical microscopy: applications in plasmonics," *Optics Express,* vol. 18, pp. 16513-16519, 2010.

[27] P. Zijlstra and M. Orrit, "Single metal nanoparticles: optical detection, spectroscopy and applications," *Reports on Progress in Physics,* vol. 74, p. 106401, 2011.